

## Growth and studies of Si-doped AlN layers

S.B. Thapa<sup>a,\*</sup>, J. Hertkorn<sup>a</sup>, F. Scholz<sup>a</sup>, G.M. Prinz<sup>b</sup>, R.A.R. Leute<sup>b</sup>, M. Feneberg<sup>b</sup>, K. Thonke<sup>b</sup>, R. Sauer<sup>b</sup>, O. Klein<sup>c</sup>, J. Biskupek<sup>c</sup>, U. Kaiser<sup>c</sup>

<sup>a</sup> Institute of Optoelectronics, Ulm University, 89081 Ulm, Germany

<sup>b</sup> Institute of Semiconductor Physics, Ulm University, 89081 Ulm, Germany

<sup>c</sup> Electron Microscopy Group of Materials Science, Ulm University, 89081 Ulm, Germany

### ARTICLE INFO

Available online 5 August 2008

#### PACS:

81.05.Ea

61.10.Nz

68.37.Lp

78.60.Hk

61.72.Ff

61.72.jd

#### Keywords:

B1. AlN

A1. Cathodoluminescence

A1. Dislocations

A1. HRXRD

A1. TEM

A1. Vacancies

### ABSTRACT

Edge-type threading dislocations (TDs) can be reduced by increasing the epilayer thickness of undoped AlN grown on *c*-plane sapphire substrate by low pressure MOVPE. Indium as a surfactant helps to reduce cracks in both, undoped and Si-doped AlN epilayers. For high Si concentrations, edge-type TDs bend and bunch together and finally emerge as V-pits on the epilayer surface. We observed an increasing intensity ratio between the deep level transitions at around 3 eV and the near-band-edge luminescence of the low temperature (10 K) CL spectra for increasing Si concentration, whereas the electrical conductivity decreased in the range of higher doping concentration. A fair electrical conductivity is obtained for a sample having moderate Si concentration of  $2 \times 10^{18} \text{ cm}^{-3}$ .

© 2008 Elsevier B.V. All rights reserved.

## 1. Introduction

AlN and  $\text{Al}_x\text{Ga}_{1-x}\text{N}$  ternary alloys have a wide application perspective especially in the area of high-power high-temperature electronic and UV optoelectronic devices. For such device applications, intentional doping is essential to achieve sufficiently large electrical conductivity and control carrier concentrations. However, only few reports have been so far published on the structural properties and transport phenomena of Si-doped AlN, due primarily to the difficulties as to the growth of high quality epilayers [1–3]. The major issues associated with poor electrical conductivity of AlN are the high ionization energy of dopants, solubility, and compensation by native defects and unintentionally incorporated background impurities [4–6].

In this study, we report on threading dislocations (TDs) in undoped AlN bulk layers of various thicknesses and on results of a crack-free 1.5  $\mu\text{m}$  thick AlN layer grown by using indium (In) as a surfactant. Impacts of Si doping on structural properties are briefly discussed. Finally, we report the effect of Si doping on the intensity of deep level transitions in low-temperature (10 K) cathodoluminescence (CL) spectra which are presumably due to

Al vacancies and/or related complexes [3] and study the electrical conductivity of the corresponding sample.

## 2. Experimental procedure

We deposited approx. 600 nm–2.5  $\mu\text{m}$  thick AlN layers on *c*-plane sapphire substrates in an AIXTRON AIX 200 RF LP-MOVPE system at 1190 °C (upper limit of our reactor) and 35 mbar in  $\text{N}_2$  and  $\text{H}_2$  ambient. Trimethylaluminum (TMAI) and  $\text{NH}_3$  were used as group III and V precursors, respectively. The details of the growth process are described elsewhere [7]. In from trimethylindium (TMIn) with a flow rate of 0.4  $\mu\text{mol}/\text{min}$  was used as a surfactant. By using silane ( $\text{SiH}_4$ ), a typically 350 nm thick Si-doped AlN layer was deposited on a 250 nm thick optimized undoped AlN buffer layer. The basic growth conditions of the Si-doped layers were similar to those of the undoped buffer layers. The surface and the crystal quality were analyzed by using atomic force microscopy (AFM) and high-resolution X-ray diffraction (HRXRD) rocking curve measurements ( $\omega$  scan with open detector). Low-temperature ( $T = 10 \text{ K}$ ) CL provided information about the spectroscopic properties. Varying high-temperature two-point *I*–*V* and room-temperature Van der Pauw–Hall measurements were carried out to measure electrical properties.

\* Corresponding author. Tel.: +49 731 5026195; fax: +49 731 5026049.  
E-mail address: [sarad.thapa@uni-ulm.de](mailto:sarad.thapa@uni-ulm.de) (S.B. Thapa).

The Si concentration [Si] and In were measured by secondary ion mass spectrometry (SIMS).

### 3. Results and discussion

The measured full width at half maximum (FWHM) of X-ray rocking curves  $\beta_{\text{hkl}}$  can be expressed as

$$\beta_{\text{hkl}}^2 = (\beta_S \cos \chi)^2 + (\beta_E \sin \chi)^2 + \frac{(2\pi/L)^2}{K_{\text{hkl}}^2}, \quad (1)$$

where  $\beta_S$  and  $\beta_E$  are the tilt (out-of-plane rotation) and the twist (in-plane rotation) angles,  $\chi$  is the angle between the reciprocal lattice vector  $K_{\text{hkl}}$  and the (001) plane, and  $L$  is the lateral coherence length [8]. The FWHMs for (002) and (102) reflections are used to estimate  $\beta_S$  and  $\beta_E$ , respectively. For simplicity, we have omitted the contribution of  $L$  and added about 20% errors in the calculations [8]. The tilt and twist of lattice planes are related to the densities  $N_S$  and  $N_E$  of the screw and/or mixed and the edge and/or mixed components, respectively, of the TDs [9]. We estimated the TD densities using well-known classical formula from Dunn and Koch [10]

$$N_S = \frac{\beta_S^2}{4.35|\mathbf{b}_S|^2}, \quad N_E = \frac{\beta_E^2}{4.35|\mathbf{b}_E|^2}, \quad (2)$$

where  $\mathbf{b}_S$  and  $\mathbf{b}_E$  are the Burgers vectors of the screw ( $\mathbf{b}_S = 0.4982 \text{ nm}$ ) and edge ( $\mathbf{b}_E = 0.3112 \text{ nm}$ ) components, respectively.

We measured an FWHM for the (002) reflection of undoped AlN samples in the range of 50 arcsec or below. The estimated value of  $N_S$ , using Eq. (2), is below  $10^7 \text{ cm}^{-2}$  for all our samples. However, as illustrated in Fig. 1, the measured FWHM for the (102) reflection strongly decreases with increasing epilayer thicknesses similar as observed by others [11]. Using Eq. (2), we calculated values of  $N_E$  approx.  $1.85 \times 10^{10}$  and  $3.6 \times 10^9 \text{ cm}^{-2}$  for the 0.6 and 2.0  $\mu\text{m}$  thick AlN epilayers, respectively. However, we observed  $N_E$  on TEM planar view investigations to be two times higher than the calculated values. From TEM cross-sectional investigations, we observe dense edge-type TDs (Fig. 2(a)) starting at the nucleation site and propagating along the layer thickness but only few screw/mixed type TDs (Fig. 2(b)). Finally, some of the edge-type TDs are bended with increasing epilayer thicknesses and annihilated with loop formation as shown in Fig. 2(a).

However, samples thicker than 1.3  $\mu\text{m}$  were not crack free. By introducing In during the growth of AlN, we obtained 1.5  $\mu\text{m}$  thick epilayers without cracks. Similarly as reported by Nicolay et al. [12], we assume that In as a surfactant changes the surface diffusion kinetics which may reduce the tensile strain and

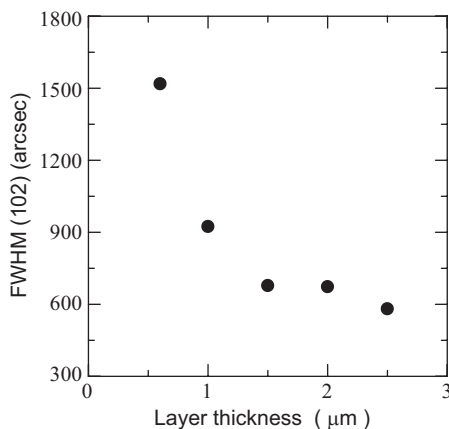


Fig. 1. Measured FWHM of X-ray rocking curve for (102) reflection.

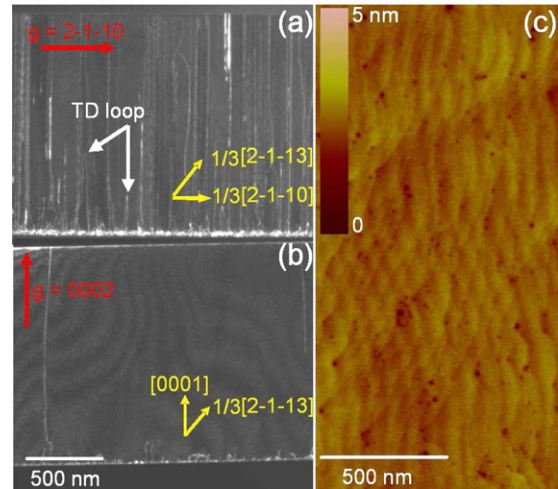


Fig. 2. TEM cross-sectional view of a 1.5  $\mu\text{m}$  thick undoped AlN epilayer grown using In showing edge-type (a) and screw-type (b) TDs. AFM image of the same sample with a measured rms surface roughness of 0.2 nm (c).

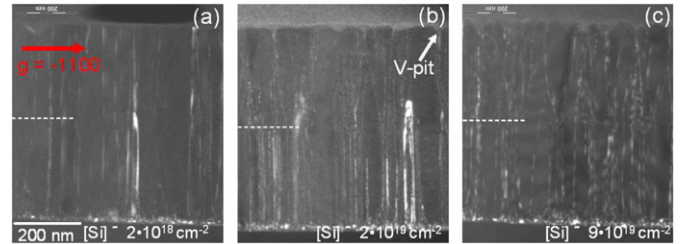
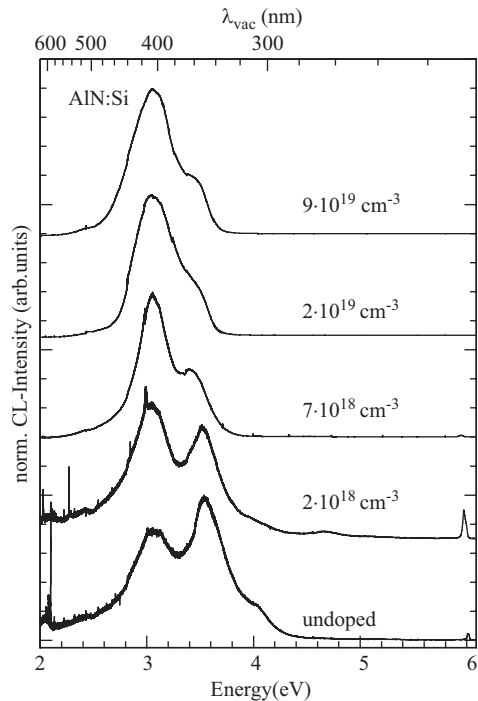


Fig. 3. TEM cross-sectional view illustrating TDs of an Si-doped layer on the top of undoped AlN (white dotted line shows the interface) where [Si]  $\approx 2 \times 10^{18} \text{ cm}^{-3}$  (a),  $2 \times 10^{19} \text{ cm}^{-3}$  (b), and  $9 \times 10^{19} \text{ cm}^{-3}$  (c). Emergence of V-pits when the TDs came closer together after bending.

eventually result in a crack-free layer. Fig. 2(c) shows an AFM image of the atomically flat surface of a sample with a measured rms surface roughness of 0.18 nm. HRXRD and TEM investigations show similar results for both AlN samples grown with and without In ambient. SIMS data showed no detectable In in the In-doped sample. Therefore, In helps to reduce cracks in AlN layers without degrading the surface and crystal quality.

SIMS depth profiles (not shown here) reveal a homogeneous incorporation of Si in the AlN epilayers up to Si concentrations of  $9 \times 10^{19} \text{ cm}^{-3}$ . TEM studies show no segregation of Si atoms in our samples for such concentrations. However, Si has adverse effects on the surface and crystal quality. Fig. 3 shows cross-sectional TEM investigations of three different doping levels, ranging from low ( $2 \times 10^{18} \text{ cm}^{-3}$ ) (a), via moderate ( $2 \times 10^{19} \text{ cm}^{-3}$ ) (b), to high ( $9 \times 10^{19} \text{ cm}^{-3}$ ) (c). The edge-type TDs, penetrating the underneath undoped layer, propagate straight to the top in the case of the low doped sample (see Fig. 3(a)), whereas they are bended at or above the interface in the case of moderate to high doping (see Fig. 3(b) and (c)). Such bending is stronger in high doping sample. The bended neighboring TDs come closer to each other, bunch together, and finally form a V-pit defect. From AFM (not shown here) and TEM investigations, we found the density, size, and depth of such pits to increase with increasing Si concentration. Relatively larger opening angles at the surface of the epilayer and deeper depth of such pits in Fig. 3(c) corroborate this argument. We speculate that the emergence of a large number of deep V-pits could also be one of the factors causing layer cracking of Si-doped samples in addition to the in-plane tensile strain [7]. Interestingly, In as a surfactant helps to reduce



**Fig. 4.** Overview of low-temperature (10 K) CL spectra, normalized to the intensity at around 3 eV, for the Si-doped and the undoped samples. The intensity ratio between the peaks about 3 eV and near-band-edge luminescence at 6 eV increases with increasing Si concentrations and minimum for  $[\text{Si}] = 2 \times 10^{18} \text{ cm}^{-3}$ .

the cracks on Si-doped layers without affecting surface and crystal quality as in the growth of undoped AlN epilayer. Similarly, instead of abrupt switching of heavy  $\text{SiH}_4$ , a slow ramping flow also helps to reduce the cracks. As opposed to the edge-type TDs, screw/mixed-type TDs are visibly annihilated at or above the interface between the doped and undoped epilayers. Meantime, new TDs are also generated in the Si-doped area (visible in TEM cross-sectional investigations not shown here). The FWHM of the (102) reflection of X-ray rocking curve are almost similar ( $\approx 1500 \text{ arcsec}$ ) in all samples. This also verifies that the edge-type TDs ( $N_E \approx 10^{10} \text{ cm}^{-2}$ ) are normally not annihilated even after strong bending and indifferent as to the Si concentration. However, the FWHM for the (002) reflection increases up to Si concentration of  $2 \times 10^{19} \text{ cm}^{-3}$  and decreases for higher concentrations [7]. We have previously reported the red-shift of near-band-edge CL peaks confirming in-plane tensile stress due to [Si] [7]. In the violet region of the CL spectra in Fig. 4, we observe two main broad peaks at about 3 and 3.5 eV which presumably are due to Al vacancies and related complexes [3,4]. The intensity ratio of these two peaks changes systematically with the Si doping, pushing up the 3 eV peak intensity at higher concentrations. This behavior is consistent with results of theoretical calculations by Mattila and Nieminen [4]. The formation energy of Al vacancies—supposed to act as triple acceptors—becomes lower than the formation energy of Al vacancy complexes for a shift of the Fermi level towards the conduction band [5,6]. From their measurements, Nam et al. [13] also deduced such a tendency and concluded, that the lower energy peak is due to Al vacancies separated by 0.5 eV from a peak assigned to Al vacancy complexes. Similarly, the intensity ratio between the deep level transitions at around 3 eV and the near band-edge luminescence at around 6 eV also changes with [Si]. It is very high for heavily doped samples.

We observe a minimum intensity ratio for the sample with  $[\text{Si}] = 2 \times 10^{18} \text{ cm}^{-3}$ . By room temperature Van der Pauw–Hall measurements, we have found fair electrical conductivity of  $0.002 \Omega \text{ cm}^{-1}$ , electron concentration of  $4 \times 10^{14} \text{ cm}^{-3}$ , and carrier mobility of  $30 \text{ cm}^2 \text{ V}^{-1} \text{ s}^{-1}$ . By varying the temperature, an activation energy of about 200 meV was estimated. High-temperature electrical measurements yield resistivities which are larger towards lower and higher Si concentrations. This corroborates the argument that Al vacancies are formed which act as triple acceptors and compensate the Si donors with increasing Si concentrations.

#### 4. Summary

We observed decreasing FWHM for the (102) reflection of X-ray rocking curves with increasing epilayer thickness of undoped AlN and measured 580 arcsec for a 2.5  $\mu\text{m}$  thick sample. Indium was used as a surfactant to get rid of surface cracking. Thus, we obtained 1.5  $\mu\text{m}$  thick high quality undoped AlN layers without any cracks. TEM studies of Si-doped samples showed the bunching of edge-type TDs causing the deterioration of the surface quality. From low temperature CL measurements, we observed that the intensity ratio between the deep level transition around 3 eV and near-band-edge luminescence with the Si concentration and found a minimum value for  $[\text{Si}] \approx 2 \times 10^{18} \text{ cm}^{-3}$ . This sample showed a fair n-type conductivity at room temperature: electron carrier concentration of  $4 \times 10^{14} \text{ cm}^{-3}$ , carrier mobility of  $30 \text{ cm}^2 \text{ V}^{-1} \text{ s}^{-1}$ , resistivity of  $530 \Omega \text{ cm}$ , and activation energy of about 200 meV for increasing temperature.

#### Acknowledgements

We like to thank M. Alomari and E. Kohn (Institute of Electron Devices and Circuits), H. Yin and P. Ziemann (Department of Solid State Physics) for high-temperature  $I$ – $V$  measurements, R. Blood and R. Rösch (Institute of Optoelectronics) for RIE, all of Ulm University; L. Kirste, T. Fuchs, and M. Grimm (Fraunhofer Institute of Applied Physics, Freiburg, Germany) for SIMS measurements; C. Kirchner (Mattson Thermal Products GmbH, Dornstadt, Germany) for high-temperature RTA, and J. Wang for AFM investigations. This work was financially supported by the Deutsche Forschungsgemeinschaft.

#### References

- [1] M. Hermann, F. Furtmayr, F.M. Morales, O. Ambacher, M. Stutzmann, M. Eickhoff, *J. Appl. Phys.* 100 (2006) 113531.
- [2] Y. Taniyasu, M. Kasu, T. Makimoto, *Appl. Phys. Lett.* 89 (2006) 182112.
- [3] Z.Y. Fan, J.Y. Lin, H.X. Jiang, *Proc. SPIE* 6479 (2007), 647911-1–11.
- [4] T. Mattila, R.M. Nieminen, *Phys. Rev. B* 55 (1997) 9571.
- [5] C. Stampfl, C.G. Van de Walle, *Appl. Phys. Lett.* 72 (1998) 459.
- [6] G. Van de Walle, J. Neugebauer, *J. Appl. Phys.* 95 (2004) 3851.
- [7] S.B. Thapa, J. Hertkorn, F. Scholz, G.M. Prinz, M. Feneberg, M. Schirra, K. Thonke, R. Sauer, J. Biskupek, U. Kaiser, *Phys. Status Solidi C* 5 (2008) 1774.
- [8] S.R. Lee, A.M. West, A.A. Allerman, K.E. Waldrip, D.M. Follstaedt, P.P. Provencio, D.D. Koleske, C.R. Abernathy, *Appl. Phys. Lett.* 86 (2005) 241904.
- [9] T. Metzger, R. Höpler, E. Born, O. Ambacher, M. Stutzmann, R. Stömmer, M. Schuster, H. Göbel, S. Christiansen, M. Albrecht, H.P. Strunk, *Philos. Mag. A* 77 (1998) 1013.
- [10] C.G. Dunn, E.F. Koch, *Acta Metall.* 5 (1957) 548.
- [11] B.N. Pantha, R. Dahal, M.L. Nakarmi, N. Nepal, J. Li, J.Y. Lin, H.X. Jiang, Q.S. Paduano, D. Weyburne, *Appl. Phys. Lett.* 90 (2007) 241101.
- [12] S. Nicolay, E. Feltin, J.-F. Carlin, M. Mosca, L. Nevou, M. Tcherynecheva, F.H. Julien, M. Ilegems, N. Grandjean, *Appl. Phys. Lett.* 88 (2006) 151902.
- [13] K.B. Nam, M.L. Nakarmi, J.Y. Lin, H.X. Jiang, *Appl. Phys. Lett.* 86 (2005) 222108.